Decomposition in alloys: an overview

M F Chisholm and D E Laughlin

Dr. M.F. Chisholm, formerly graduate student at Carnegie Mellon University, is currently at IBM, Yorktown Heights, NY 10598. Professor D.E. Laughlin is in the Department of Metallurgical Engineering and Materials Science at Carnegie Mellon University, Pittsburgh, PA 15213

Synopsis

In this paper we first review two methods of modeling decomposition of alloys within a miscibility gap. These methods are termed the "cluster kinetics" techniques and the "phenomenological diffusion" models. We note that the classical presentations of these models best describe the extremes in decomposition behavior, near the solvus and very far from the solvus, respectively. We then review some recent simulation and experimental studies of decomposition of Cu-Co alloys in regions of the phase diagram that can not be quantitatively modelec *via* the *classical* techniques. We show that the *qualitative* features of both the cluster kinetics behaviors and phenomenological diffusion behaviors appear in this region. This demonstrates a continuity of mode of decomposition throughout the miscibility gap.

Introduction

It is well known that the decomposition behavior of a supersaturated solid solution within a miscibility gap depends strongly on its degree of supersaturation. At small supersaturations, the precipitates of the new phase appear randomly throughout the grains of the alloy with compositions that approach their equilibrium ones. On the other hand for large supersaturations, the new phase appears homogeneously throughout the grains, originating with compositions that are not very different than the matrix phase from which they form.

Many reviews exist on the decomposition of alloys within a miscibility gap. (1-5) The review of Martin (1) points out that the theories that have been developed to model such decomposition fall into two main classes: (a) those that deal at the microscopic level, looking at the attachment/detachment rate and (b) those that deal at a more macroscopic level, looking at the average flux of solute in the system. Herein, we will call these the *cluster kinetics models* and *phenomenological diffusion models*, respectively. The *cluster kinetics* approach is usually used by investigators to model the decomposition behavior at small supersaturations, while the diffusion models are usually used to model decomposition at large supersaturations. Both models can, in principle, be used to model decomposition over the entire range of supersaturations. However, the *classical presentations* of these models include assumptions that limit their applicability to a limited region of the phase diagram.

Cluster Kinetics Models

The cluster kinetics model (1) offers a microscopic description of decomposition. Part of this description is based on the fact that atoms have to overcome an energy barrier to change their position. Atomic diffusion occurs when atoms on neighboring sites exchange positions or move into a neighboring vacant site. The energy for these biatomic fluctuations is supplied by thermal vibrations. An important concept is that of the binding energy of an atom in various arrangements in the crystal. When all but the configurational contributions can be ignored, the binding energy determines the solute-solvent atom arrangements. When like-atom bonds are energetically favorable, there is a tendency for the solute atoms to cluster. The natural tendency for the system to achieve maximum randomness (entropy) opposes the clustering reaction. Gibbs used a different (but equivalent) and more widely used approach to address the question of the formation and stability of a different phase within any homogeneous "fluid". In his approach the work of formation consists of two opposing terms. The creation of the new phase results in a negative contribution, proportional to the volume of the new phase created, and a positive contribution (opposing the cluster formation), proportional to the surface area created. Using Gibbs' ideas on the work of formation of a critical cluster, Volmer and Weber (6) produced the first satisfactory theory of nucleation. Although the original theory was developed for the condensation of vapor, it has since been improved and applied to other types of phase changes. In 1938, Becker (7) first applied the

theory of nucleation to transformations in binary systems.

Phase decomposition in the cluster kinetics models can be described generally by a master equation of the form (8,1):

$$\frac{\partial P(n,t)}{\partial t} = -\sum_{n'} \left[W(n \rightarrow n') P(n,t) + W(n' \rightarrow n) P(n',t) \right] \qquad [1]$$

where P(n,t) is the probability that the variable of interest, e.g. the cluster size, has the value n at time t, and W(n n') is the probability that a transition from cluster size n to n' occurs in unit time.

Various approximations are made to simplify the equation. The *classical* nucleation equation can be obtained by assuming:

(a) only biatomic reactions occur
(b) a constant number of each size cluster exists
(c) only the critical cluster can form.

Using these physical assumptions, the mathematical expressions simplify to the well-known *classical nucleation* rate equation

$$J = ZW^*N \exp\left(\frac{-\Delta F^*}{kT}\right) \qquad [2]$$

where N is the number of lattice sites, W* is the rate at which an atom attaches to a critical cluster, Z is the Zeldovich factor and ΔF^* is the free energy of formation of the critical nucleus. See Martin (1) or Christian (2) for a derivation of this equation.

The term *classical* is used here to denote nucleation theories based on the concept of a *critical cluster*. Within this general category there have been improvements to the original Becker treatment through the use of more realistic thermodynamic expressions for the free energy and interfacial energy. In Becker's treatment it is assumed that the nucleus has the same composition it would have as a stable phase, that it is internally uniform and that the composition at the matrix : nucleus interface changes discontinuously. From these assumptions the interfacial energy is a constant. The most serious objection to this treatment is the assumption of a sharp interface. This shortcoming was addressed and the result applied to nucleation by Hillert (9,10) and by Cahn and Hilliard (11,12). Hillert's treatment is based on the calculation of the free energy of the composition variation across an interface in a one dimensional discrete lattice. Cahn and Hilliard extended the treatment of nucleation to three dimensions using a continuum model. A recent study of nucleation by LeGoues and Aaronson (13,14) used a three dimensional discrete lattice model proposed by Cook, de Fontaine and Hilliard (15). This discrete model, based on the treatment of Cahn and Hilliard, removes the continuum approximation and the limitations it places on the study of real crystals.

The quantitative features of classical nucleation theory will not be valid when the alloy in question departs from conditions that are accurately portrayed by the three assumptions listed above. This occurs for values of ΔF^* less than $\sim$ 10 kT. In this region other non-critical decomposition paths have *similar* thermodynamic barriers so that the alloy will decompose along paths that do not exactly minimize the work of formation of the new phase. (16,17,18)

Phenomenological Diffusion Equation

The diffusion equation approach provides a macroscopic description of the decomposition process. Here, the gradient of the chemical potential is assumed to act as the driving force for the flux of solute atoms. From this assumption, a general macroscopic diffusion equation is derived:

$$\frac{\partial}{\partial t} c = M \left[\nabla \left(\frac{\partial^2 f}{\partial c^2} \nabla c \right) - 2K \nabla^4 c \right] \qquad [3]$$

where M is the mobility, and K is the gradient energy. See Hilliard (4) for a derivation. This equation also assumes that the path of decomposition will be the most probable one, *viz.* the one with the minimum work of formation.

This 'general' diffusion equation has been obtained assuming that the system will follow the most probable decomposition path (minimum work of formation). No fluctuations from this path are considered. It is also assumed that the composition variation in the inhomogeneous system is diffuse compared to the range of intermolecular forces, so that only a single gradient energy term needs to be considered. The final assumptions are that the mobility and the gradient energy coefficients are independent of composition.

Cahn (19) linearized this equation in order to obtain analytic solutions. The result is the linear first order differential equation

$$\frac{\partial}{\partial t} c = M \left[\frac{\partial^2 f}{\partial c_o^2} \nabla^2 c - 2K \nabla^4 c \right] \qquad [4]$$

Solutions to this equation yield a periodic distribution of solute. Furthermore, if elastic anisotropy is included, the modulations in solute are predicted to be aligned along the elastically soft directions. (20) The wave of fastest growth is the one for which:

$$\lambda_m = 2\pi \left[\frac{-4K}{\left(\frac{\partial^2 f}{\partial c^2} \right)} \right]^{1/2} \qquad [5]$$

Thus, this approximation to the model can be seen to be valid only within the spinodal, where the denominator is negative. In fact, as the spinodal is approached, the value of λ_m diverges.

It can be seen, therefore, that the *classical approximations* to both the cluster kinetics and phenomenological diffusion equation break down near the spinodal. However, if the various approximations were not made, the models should still be valid. In this investigation, we chose to examine the decomposition of alloys near the mean field spinodal.

We do this experimentally in the Cu-Co system and we model such decomposition by the techniques of Monte Carlo simulation (See 21). The details of the work are to be published elsewhere. Herein we briefly summarize the major findings as they impact on the various models of decompcsition.

Alloys

We chose to study decomposition in Cu-Co because the new phase is the same structure as the matrix phase (fcc), there is only a small atomic misfit ($\approx$ 1.2%). In addition, information on the phase boundaries, thermodynamics, precipitation reactions and diffusivity exists. We modeled (on the basis of a subregular solution) the free energy of the solid solution which reproduced the phase diagram, and used this free energy to calculate *via* the Cahn-Hilliard approach the locus of points on the phase diagram with various constant values of ΔF^*, the minimum work to form a stable nucleus. See Figure 1. This allowed us to choose the alloys and temperatures of isothermal aging with values of $\Delta F^* < 10$ kT.

Monte-Carlo Results

Using the appropriate values of interaction energy *etc.* the decomposition process in a volume 24 x 24 x 24 unit cells in dimension was simulated. The process for various times is shown in Figure 2, for a 3% solute alloy. Notice that at t=0, the solute appears random and with aging time some regions get darker. This is equivalent to an increase in composition of the "particles". Also notice that with time, the radius of the particles increases. The particles are initially irregular shape; with time they become more equiaxed. This decomposition process looks "continuous" in that the particles *continuously* form from the solid solution with *continuous* change in composition and shape. However the decomposition took place above the mean field spinodal. Thus, we see that the process "looks like" spinodal decomposition, even though we know it is occurring outside of the spinodal region. Of course, the direct space observation of the decomposing alloy is not very quantitative. Thus, we calculate the pair correlation function (Γ) for each decomposition time and *via* the structure function S (the Fourier transform of Γ) the simulated intensity near the origin of reciprocal space can be calculated. It is the structure function which can be experimentally measured. The structure function is directly proportional to the measured intensities from small-angle scattering experiments. This is shown in Figure 3 for the 3% alloy. This figure shows that the solute in as quenched "alloy" is indeed random, since the curve is flat. It also shows that the correlation distance between enriched regions is increasing with time (i.e., coarsening occurs: see also Figure 2).

This behavior is different than that expected when phase separation occurs in the regions where the classical theories of nucleation and spinodal decomposition can be applied. With classical homogeneous nucleation, decomposition occurs through the formation of clusters with the lowest interfacial energy. For the case of isostructural decomposition (with no misfit) investigated herein, these clusters would be equiaxed from the beginning of the process, because interfacial energy dominates the determination of the shape of the emerging nuclei. Classical spinodal decomposition occurs by the exponential growth of a dominant (maximum amplification rate) wavelength. This results in an interconnected structure with two interpenetrating regions; one enriched in solute, one depleted in solute. In both of these cases, which represent extremes in behavior, a single path dominates the decomposition process. This is not true when the barrier to decomposition is small. With spinodal nucleation, fluctuations in composition can become supercritical along several paths. There is enough thermal energy so that the cluster with the minimum work of formation is not the only cluster that will form. The most probable evolution (that with the lowest work of formation) does not dominate the phase separation process in the spinodal nucleation region. The kinetics of the decomposition reaction also plays a role. As can be seen in the atomic distributions, the irregularly shaped regions which form initially do not have the lowest possible interfacial energy for a given precipitate volume. They exist because they have formed faster than the critical cluster. The barrier to form these irregular particles is small enough that the thermal energy in the system is sufficient to allow decomposition along several paths.

Small Angle Neutron Scattering

Small Angle Neutron Scattering experiments using 0.75 nm wavelength neutrons were carried out at the National Bureau of Standards. This wavelength was large enough to eliminate double diffraction. As is well known, small angle investigations study the composition fluctuations *via* the differences in atomic scattering, not strain, as the effect of strain is negligible about the transmitted beam. A single crystal was used as well as polycrystalline material. The scattering from the single crystal (2.5 %Co) aged for various times at 723 K is shown in Figure 4. The first pattern 4a, is from the as-quenched sample and shows little scattering. In 4b, the scattering is anisotropic and aligned along the <100> directions. This effect is less in 4c. After 24 hours (4d) the scattering is nearly isotropic and a distinct small-angle scattering peak is observed.

The observed scattering is due to the cobalt-enriched regions which are forming during the decomposition process. The elongation of the SANS patterns (Figures 4(b) and (c)) arises from shape effects. We propose that the particles are platelike with their thin directions perpendicular to (100). With time, the particles become more equiaxed and a correlation in spacing appears. (See Figure 4(d).) An interpretation consistant with the Monte Carlo results is that initially, cobalt enriched regions are formed. The shape of these regions is influenced by the elastic properties of the alloy. The effect of elastic anisoptropy was not taken into account in the Monte Carlo simulations. With increasing aging time at 723 K, distinct spherical cobalt-rich precipitates develop and coarsen, resulting in a fairly constant interparticle spacing.

Polycrystalline samples of Cu-Co were also studied by SANS. The 1% alloy showed no peak until 24 hours at 723 K, while the 2% alloy showed no peak until 2.5

hours at 723 K. The 3% alloy showed correlations after only 10 minutes at the same aging temperature. See Figure 5. These results can be compared directly to the Monte Carlo simulated decomposition for the 3% alloy. See Figure 3. The wavelength of correlation of the alloys is seen to be 3.6 nm for the experimental alloys and 3.3 nm for the simulated alloy. This is a rather good fit, when it is remembered that there was only one adjustable parameter used in simulation, namely the interaction energy. This adjustable parameter was chosen so as to best reproduce the experimental phase boundary.

Transmission Electron Microscopy

Samples with less than 3% Co showed no signs of decomposition on the quench. The 4% Co alloy showed only strain modulations in the microstructure; no particles were imaged. The 5.4% Co alloy had particles of diameter 5-6 nm present in the as quenched condition.

When examining the 4% Co alloy aged 3 hours at 823 K using the two beam technique, a heavily modulated structure is imaged (see Figure 6a). These modulations are aligned along the <100> directions. However, when the alloy was imaged using the symmetric multibeam technique a large number of distinct particles were seen (Figure 6b). The modulations, in this case, are due to interactions between the elastic strain fields of the precipitates (*v/z.* net matrix strain contrast) (21).

Electron microscopy revealed both <100> modulations and individual precipitates, depending on the diffraction conditions in samples of the 2.54 at% cobalt alloy aged for more than two hours at 723 K. For aging times less than two hours, aligned modulations in contrast were observed but no precipitates were imaged (See Figure 7a and 7b). Diffuse scattering is observed in selected area electron diffraction patterns from the 2.54 at% alloy. The diffuse intensity is also aligned along the <100> directions and becomes more obvious with increasing aging time (See Figure 8). The diffuse scattering is interpreted to be the result of the distortion of the lattice caused by the precipitation of cobalt-enriched regions (*i.e.* Huang scattering, 22).

Summary of Results

The decomposition reaction of Cu-Co alloys at temperatures near the spinodal follows a complex path. Initially, irregularly shaped and randomly located Co-enriched regions form. Their non-equiaxed shape gives rise to the anisotropic scattering observed by SANS. The lattice distortion caused by the formation of the cobalt-enriched regions results in the diffuse scattering observed by electron diffraction and the aligned modulations imaged by TEM. With time the particles grow and are further enriched in solute. Eventually, the particles become correlated as observed by the small angle peak in SANS.

Thus, the decomposition of alloys near the spinodal occurs in a fashion that has *some* features predicted by either the classical spinodal decomposition treatments or classical nucleation models. However, the quantitative features are described by neither. These *classical* treatments describe the most probable decomposition path, from the point of view of the thermodynamics. However, the decomposition process is a kinetic process, controlled (for diffusional phase transformations) by the heat bath in contact with the system which induces random changes in atomic positions. The neglect of these random fluctuations is most serious near the spinodal. The simulations demonstrate the role that kinetics plays in solutions with small barriers to decomposition. The most probable change does not always occur when the differences between it and other possible paths is small.

Acknowledgements

We wish to thank the National Science Foundation for financial support of this work (DMR-84-13115). Also, we acknowledge with thanks many critical discussions with William A. Soffa.

REFERENCES

1. G. Martin, in *Solid State Phase Transformations in Metals and Alloys, Les Editions de Physique*, Orsay, France, 337 (1979)
2. J.W. Christian, *The Theory of Transformations in Metals and Alloys*, Pergamon Press, Oxford (1975).
3. J. W. Cahn, *Trans. TMS-AIME*, 242, 166 (1968).
4. J. Hilliard, in *Phase Transformations*, ASM, 497 (1970).
5. D. de Fontaine, in *Ultrafine-Grain Metals*, ed. J.J. Burke and V. Weiss, Syracuse U. Press, Syracuse, NY, 93 (1970).
6. M. Volmer and A. Weber, *Z. Physik. Chem.*, 119, 277 (1925).
7. R. Becker, *Ann. Phys.*, 32, 128 (1938).
8. L. Farkas, *Z. Physik. Chem.*, 125, 239 (1927).
9. M. Hillert, Sc.D. Dissertation, MIT, (1956).
10. M. Hillert, *Acta Met.*, 9, 525 (1961).
11. J. W. Cahn and J.E. Hilliard, *J. Chem. Phys.*, 28, 258 (1958).
12. J.W. Cahn and J.E. Hilliard, *J. Chem. Phys.*, 31, 688 (1959).
13. F.K. LeGoues and H.I. Aaronson, *Acta Met.*, 32, 1837 (1984).
14. F.K. LeGoues and H.I. Aaronson, *Acta Met.*, 32, 2241 (1984).
15. H.E. Cook, D. de Fontaine and J.E. Hilliard, *Acta Met.*, 17, 765 (1969).
16. D. de Fontaine, *Trans. Met. Soc. AIME*, 245, 1703 (1969).
17. J.S. Langer, *Ann. Phys.*, 65, 53 (1971).
18. K. Binder, C. Billotet and P. Mirold, *Z. Physik.*, B30, 183 (1978).
19. J.W. Cahn, *Acta Met.*, 9, 795 (1961).
20. J.W. Cahn, *Acta Met.*, 10, 179 (1962).
21. J.L. Lebowitz, J. Marro and M. H. Kalos, *Acta Met.*, 30, 297 (1982).

22. J.A. Cornie, A. Datta and W.A. Soffa, *Met. Trans.*, 4, 727 (1973).

23. K. Huang, *Proc. Roy. Soc. Lond.*, A190, 102 (1947).

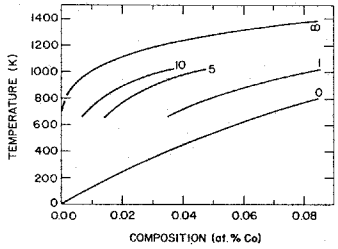

Figure 1. Iso-energy lines of the work to form a critical nucleus in Cu-Co alloys, using the Cahn-Hilliard analysis (11,12).

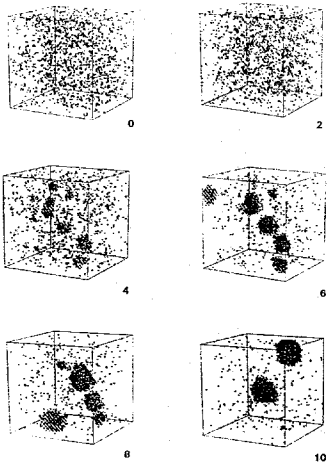

Figure 2. Monte Carlo simulation of the atomic distribution in a Cu-3at.%Co alloy after various aging times at 723 K. The numbers are proportional to the number of exchange attempts per site (e.g. 10 corresponds to 40,550 attempts per site).

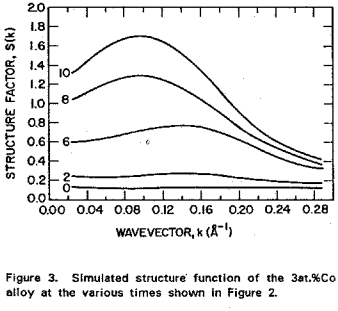

Figure 3. Simulated structure function of the 3at.%Co alloy at the various times shown in Figure 2.

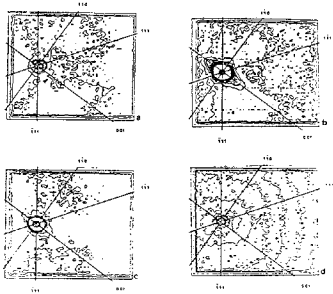

Figure 4. Iso-intensity lines of the small-angle scattering pattern from a single crystal Cu-2.54 at.% Co alloy aged at 723 K. The [110] crystal axis is parallel to the neutron beam. λ=7.5 A. Sample to detector distance - 2.0 m. (a) As-quenched sample. (b) Sample aged 30 min. Scattering is anisotropic, the intensity is strongest along the <100> directions. (c) Sample aged 2 hours. Anisotropy of scattering is less pronounced. (d) Sample aged 24 hours. Scattering is isotropic. A small-angle scattering peak (ring) is present at small wavevectors.

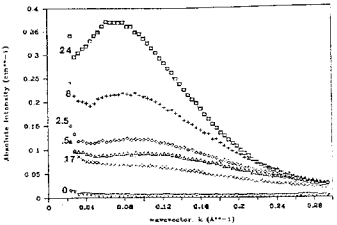

Figure 5. Radial averaged scattering cross-sections (absolute units) for the 3 at.% Co alloy aged for various times (hours) at 723 K. The scattering has a peak after only 10 minutes of aging. The scattering peak grows and shifts to smaller wavevectors as the aging time for the samples is increased.

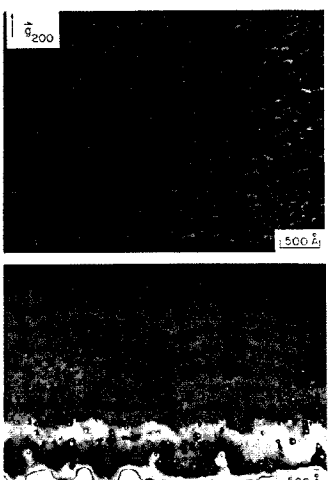

Figure 6. 4 at.% Co alloy aged at 823 K for 3 hours. (a) Operating reflection is (200), the direction of g is as marked. Modulations in contrast are aligned along the <100> directions (b) Symmetric multi-beam condition ([100]*Z.A.). The <100> directions are along the vertical and horizontal axes of the photo.

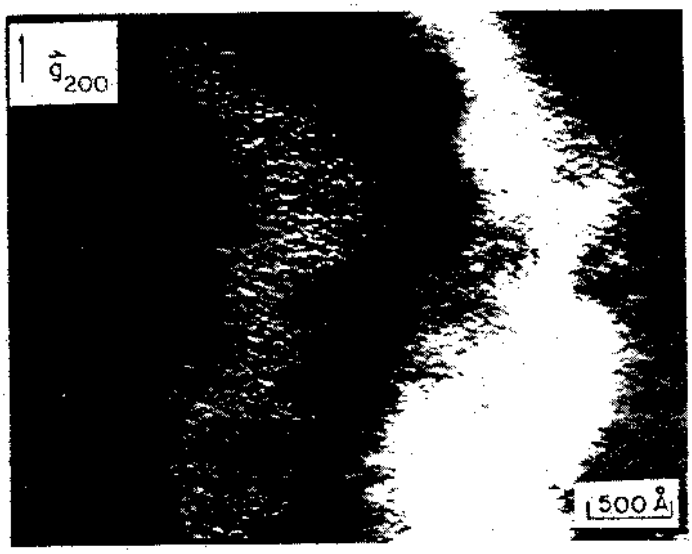

Figure 7. 2.54 at.% Co alloy aged at 723 K for 2 hours. (a) Operating reflection is (200), the direction of g is as marked. (b) Symmetric multi-beam condition ([100]*Z.A.). No precipitates are imaged.

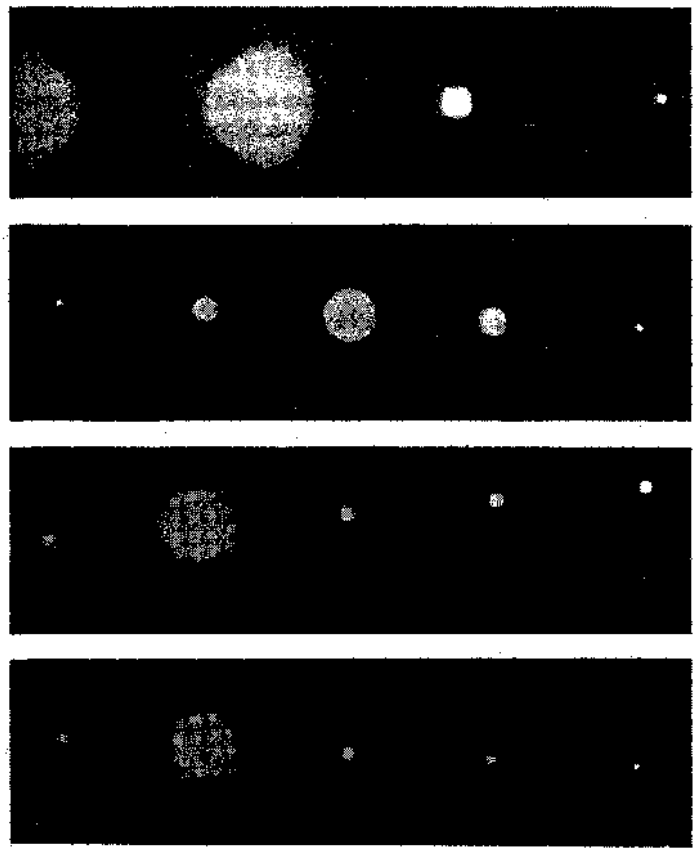

Figure 8. Electron diffraction effects along the <100> direction for a 2.54 at.% Co alloy aged for (a) 24 hours, (b) 2 hours, (c) 30 minutes, (d) as-quenched.